FULL PAPER

BJC

British Journal of Cancer (2016) 114, 905–916 | doi: 10.1038/bjc.2016.6

Keywords: breast cancer; preclinical models of cancer; ROS modulation; novel flavonoids; animal models of cancer; natural products; SAR studies; xenograft models; novel antitumour agents

Antitumour activity of the novel flavonoid Oncamex in preclinical breast cancer models

Carlos Martínez-Pérez*[,1], Carol Ward[1], Arran K Turnbull[1], Peter Mullen[2], Graeme Cook[3], James Meehan[1], Edward J Jarman[1], Patrick IT Thomson[4], Colin J Campbell[4], Donald McPhail[3], David J Harrison[2] and Simon P Langdon[1]

[1]*Division of Pathology Laboratories, Institute of Genetics and Molecular Medicine, University of Edinburgh, Western General Hospital, Edinburgh EH4 2XU, UK;* [2]*School of Medicine, University of St Andrews, St Andrews KY16 9TF, UK;* [3]*Antoxis Limited, IMS Building, Foresterhill Health and Research Complex, Aberdeen AB25 2ZD, UK and* [4]*EaSTCHEM, School of Chemistry, University of Edinburgh, Joseph Black Building, Edinburgh EH9 3FJ, UK*

Background: The natural polyphenol myricetin induces cell cycle arrest and apoptosis in preclinical cancer models. We hypothesised that myricetin-derived flavonoids with enhanced redox properties, improved cell uptake and mitochondrial targeting might have increased potential as antitumour agents.

Methods: We studied the effect of a second-generation flavonoid analogue Oncamex in a panel of seven breast cancer cell lines, applying western blotting, gene expression analysis, fluorescence microscopy and immunohistochemistry of xenograft tissue to investigate its mechanism of action.

Results: Proliferation assays showed that Oncamex treatment for 8 h reduced cell viability and induced cytotoxicity and apoptosis, concomitant with increased caspase activation. Microarray analysis showed that Oncamex was associated with changes in the expression of genes controlling cell cycle and apoptosis. Fluorescence microscopy showed the compound's mitochondrial targeting and reactive oxygen species-modulating properties, inducing superoxide production at concentrations associated with antiproliferative effects. A preliminary *in vivo* study in mice implanted with the MDA-MB-231 breast cancer xenograft showed that Oncamex inhibited tumour growth, reducing tissue viability and Ki-67 proliferation, with no signs of untoward effects on the animals.

Conclusions: Oncamex is a novel flavonoid capable of specific mitochondrial delivery and redox modulation. It has shown antitumour activity in preclinical models of breast cancer, supporting the potential of this prototypic candidate for its continued development as an anticancer agent.

Flavonoids account for the largest and most ubiquitous group of plant secondary metabolites. They comprise seven different subclasses of polyphenols with a common backbone consisting of two fused rings linked to another aromatic ring (Weng and Yen, 2012). Beyond their numerous roles in plant biology, flavonoids have long been identified as possessing a wide range of bioactivities, including protective and therapeutic effects against cancer, cardiovascular and neurodegenerative diseases, and thus have great potential for clinical application (Romano *et al*, 2013).

In particular, extensive preclinical evidence has accumulated for their antiproliferative effects against several types of cancer, including breast (Pan *et al*, 2012), prostate (Brown et al, 2005), lung (Park *et al*, 2012) and colorectal cancers (Ko *et al*, 2005a). However, their use in a therapeutic context is presently hampered by poor drug-like attributes resulting in low bioavailability and metabolic stability, limited cell uptake and ineffective delivery to important cellular compartments such as the mitochondria.

*Correspondence: C Martínez-Pérez; E-mail: c.martinez@sms.ed.ac.uk

Revised 17 November 2015; accepted 16 December 2015; published online 31 March 2016

Previous research has reported the anticancer effect of flavonoids on breast tumours through multiple mechanisms (Martinez-Perez *et al*, 2014). Structural similarities to the hormone 17β-oestradiol allow for interaction with the oestrogen receptors (ERs) (Limer and Speirs, 2004), although the effect is predominantly beneficial due to a stronger affinity for the proliferation-inhibiting isoform ERβ (Ström *et al*, 2004; Harris *et al*, 2005; McCarty, 2006). In addition, flavonoids can block the bioactivation of procarcinogens (Ciolino and Yeh, 1999; Moon *et al*, 2006) and act as inhibitors for oestrogen-producing and metabolising enzymes (Sanderson *et al*, 2004; Rice and Whitehead, 2006) and for the breast cancer resistance protein (BCRP), involved in the development of multidrug resistance (Katayama *et al*, 2007; Tan *et al*, 2013).

Flavonoids exert these antitumour activities in a concentration- and time-dependent manner, and have been shown to be effective in the treatment of numerous cancer types specifically targeting malignant cells (Ramos, 2007). Such properties support flavonoids as strong candidates for the development of novel anticancer treatments. Indeed, research has shown that administration of flavonoids can lead to a decrease in inflammation, proliferation, tumour size and metastasis (Limer and Speirs, 2004; Peluso *et al*, 2013). Further potential lies in their application as re-sensitisers in tumours clinically resistant to TRAIL (tumour necrosis factor-related apoptosis-inducing ligand) (Siegelin *et al*, 2009), radiotherapy (Yi *et al*, 2008), endocrine therapy (Mai *et al*, 2007; Tu *et al*, 2013) or chemotherapeutic agents like Centchroman (Singh *et al*, 2012).

The flavonol myricetin is a natural flavonoid with powerful antioxidant activity that has been shown to have a therapeutic effect in different cancers both *in vitro* and *in vivo*. It exerts apoptotic effects in combination with TRAIL (Siegelin *et al*, 2009) or by other mitochondrial-dependent pathways (Ko *et al*, 2005b), as well as inducing G_2/M cell cycle arrest (Zhang *et al*, 2008). We hypothesised that myricetin-derived, synthetic flavonoids with improved antioxidant properties, specific mitochondrial targeting and optimised physicochemical properties and drug-like attributes (McPhail *et al*, 2009) may have enhanced potential as antitumour agents.

In this study, we characterise a small library of these myricetin-derived new chemical entities. We assessed their antitumour properties in a panel of breast cancer cell lines, describing structure–activity relationships (SARs) and investigating the mechanism of action of these compounds, including the role of reactive oxygen species (ROS) modulation in their antitumour effects. The potential application of such synthetic derivatives in an *in vivo* setting was also assessed in a human breast cancer xenograft model.

MATERIALS AND METHODS

Cell culture. Breast cancer cell lines MCF-7, MDA-MB-231, BT-549 and HBL-100 (all obtained from ATCC) were cultured in Dulbecco's Modified Eagle Medium (DMEM) supplemented with 10% heat-inactivated foetal calf serum (FCS) and 100 IU ml^{-1} penicillin/streptomycin. These cell lines correspond to different molecular subtypes of breast cancer, with hormone-dependent MCF-7 expressing ERs (ER+) and MDA-MB-231, BT-549 and HBL-100 being characterised as triple-negative cell lines, lacking in receptors for oestrogen, progesterone and human epidermal growth factor (ER− PR− HER2−) and, hence, hormone-independent. The LCC1, LCC2 and LCC9 (hormone-independent cells established by derivation of selected subpopulations of MCF-7 cells (Brünner *et al*, 1993b, 1997; Thompson *et al*, 1993)) were cultured in phenol red-free DMEM supplemented with 5% heat-inactivated FCS charcoal-stripped of steroids. Cells were incubated at 37 °C in a humidified atmosphere containing 5% CO_2. Cells were grown to confluence with periodic medium changes and collected by brief incubation with trypsin/ethylenediaminetetraacetic acid solution. All cell lines were authenticated by short tandem repeat profiling undertaken by the Public Health England (Salisbury, UK) in December 2014.

Sulforhodamine B assay. Cells (500–2000 cells per well, depending on doubling time) were typically plated in 96-well microplates, and medium changed to 2.5% FCS DMEM after 24 h, following preliminary experiments that showed an improved effect of drugs for lower serum concentrations (Supplementary Figure 1). Cells were treated after a further 24 h with a library of eight compounds, including myricetin and lead compounds AO-1530 and Oncamex (Table 1). Treatments included a range of micromolar concentrations between 0.01 and 100 μM for all compounds. Each experiment was repeated at least once.

After treatment cells were fixed with 50 μl per well of cold 25% trichloroacetic acid for 1 h at 4 °C and washed 10 times with H_2O. After drying, plates were stained for 30 min with 50 μl per well of 0.4% (w/v) sulforhodamine B (SRB) (in 1% acetic acid) and washed four times with 1% acetic acid. Protein-bound SRB was solubilised in 150 μl per well of 10 mM Tris solution (pH 10.5), followed by measurement of optical density (OD) at 540 nm in a BP800 Microplate Reader (Biohit, Helsinki, Finland). Results were processed, subtracting average values of blanks and day 0 controls and normalising to untreated controls.

Fluorescence microscopy. Cells were grown on coverslips and treated with Oncamex for 15 min, 1 or 6 h at 37 °C, adding 25 nM Mitotracker Deep Red (Life, Eugene, OR, USA) for the last 30 min (or 15 min for the shortest incubation). Cells were fixed in 4% parafarmoldehyde for 45 min, washed three times in phosphate-buffered saline (PBS) and allowed to air-dry before mounting on Superfrost Plus microscope slides (Thermo Scientific, Braunschweig, Germany) using ProLong Gold antifade mountant with DAPI (4′,6-diamidino-2-phenylindole, Life, Bleiswijk, Netherlands). Oncamex possesses fluorescent properties, with a stable signal measurable at 550 nm_{EXC}/570 nm_{EM}. Cells were visualised, captures obtained and analysed using a PM-2000 AQUA (Automated Quantitative Analysis) system (HistoRX, New Haven, CT, USA) and an Axioplan 2 fluorescence microscope (Zeiss, Cambridge, UK).

The production of ROS was detected by fluorescence microscopy. The method above was followed with additional staining of cells with mitochondrial probes following the manufacturers' guidelines, incubating with 10 μM MitoPY1 (Tocris, Bristol, UK) or 2.5 μM MitoSOX (Life) to detect mitochondrial production of hydrogen peroxide and superoxide, respectively.

Cell spotting. A total of 10^5 MCF-7 cells per well were plated in triplicate in six-well plates. After treatment and incubation, cells were trypsinised and centrifuged for 5 min at 2000 r.p.m. Resulting pellets were resuspended in 100 μl of FCS and transferred to Cytofunnels EZ Single (Fisher, Braunschweig, Germany) mounted on Superfrost Plus slides (VWR International, Leuven, Belgium) to be spun for 3 min at 500 r.p.m. in a Cytospin 4 Cytocentrifuge (Thermo Fisher, Chesire, UK). Slides were allowed to air-dry and stained using the Reastain Quick Diff kit (Reagena, Toivala, Finland), to fix and dye both protein and DNA. After rinsing and air-drying, cells were observed on an Olympus BX51 microscope (Olympus, Hamburg, Germany) and images were captured using the software package Q-Capture Pro (Q Imaging, Surrey, BC, Canada).

Plate-based assays. The CellTox Green Cytotoxicity and ApoTox-Glo Triplex assay kits (Promega, Madison, WI, USA) were used to measure cytotoxicity at different timepoints and to assess the

Table 1. Library of novel flavonoids screened for their antitumour properties

Compound	Structure	Characteristics/properties
Myricetin	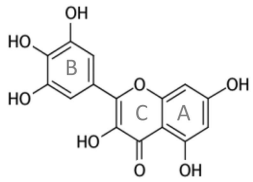	Naturally occurring flavonoid identified as particularly powerful antioxidant
AO-1530	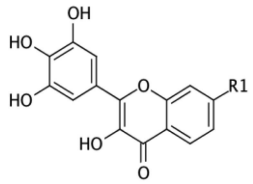	Myricetin-based novel flavonoid, mitochondria-targeted and with active redox properties. Non-redox-active OH groups removed and a decyl chain similar to the one found in vitamin E has been added to improve permeability and targeting
Oncamex (R1)	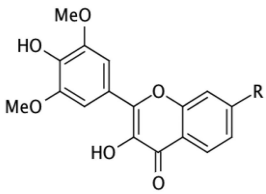	Bi-methoxylated second-generation analogue of AO-1530
AO-1486 (R2)		Same backbone as AO-1530, but nonspecific targeting
AO-1487 (R3)		Same backbone as AO-1530, but nonspecific targeting
AO-594 (R4)		Same backbone as AO-1530, but weaker specificity for the mitochondrial compartment
AO-155-179	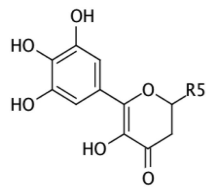	Similar backbone to that of AO-1530 but one of the fused rings has been removed, leaving a less flavonoid-like structure
AO-714A	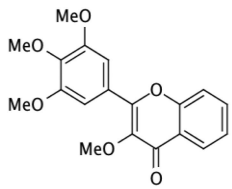	Fully blocked redox activity
AO-594	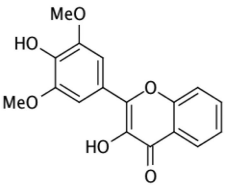	Same backbone as AO-1530, but nonspecific targeting

Abbreviations: R1 = $(CH_2)_9$-CH_3; R2 = $(CH_2)_3$-NH-$(CH_2)_4$-NH_2; R3 = CH_2-(C_6H_8)-NH_2.HCl; R4 = no radical; R5 = $(CH_2)_{10}$-CH_3. The addition of different moieties and radicals granted distinctive redox potential and intracellular targeting to analogues in a library of seven novel, myricetin-derived flavonoids.

mechanism of action of the drugs studied, respectively. In all, 10^4 cells per well were plated in 96-well microplates (black walls for CellTox assay and white for ApoTox), changing the medium to phenol red-free DMEM after 24 h. The protocols were carried out following the manufacturer's instructions, and fluorescence and luminescence were measured in a Labsystems Fluoroskan Ascent FL (Thermo, Vantaa, Finland) plate reader.

Cell lysates. In all, 3×10^6 MCF-7 cells per dish were plated in 140-cm^2 Petri dishes. After treatment, cells were washed in PBS and incubated for 10 min on ice in 400 μl of lysis buffer (50 mM Tris, 5 mM EGTA and 150 mM NaCl) containing Complete Protease Inhibitor Tablet (Roche, Mannheim, Germany; 1 tablet per 10 ml), 1 : 100 of phosphatase inhibitor cocktails 2 and 3 (Sigma, St Louis, MO, USA), 1 : 200 aprotinin (Sigma) and 1 : 100

Triton X (Sigma). Lysates were centrifuged at 13 000 r.p.m. at 4 °C for 6 min. Supernatants were recovered and stored at −70 °C.

Bicinchoninic acid assay. Protein concentration in cell lysates was determined by bicinchoninic acid (BCA) assay. Bovine serum albumin (BSA, G Biosciences, St Louis, MO, USA) was used as protein standard, preparing serial dilutions (0–1000 $\mu g\,ml^{-1}$) in distilled water (dH_2O), while aliquots of cell lysates were also diluted 1 : 10 in dH_2O. A volume of 1 ml of a 1 : 50 copper sulphate : BCA solution was added to 50 μl of each protein solution in borosilicate glass tubes. Tubes were incubated at 60 °C for 15 min before cooling briefly and dispensing replicates of each solution to a 96-well microplate. The OD at 540 nm was measured in a BP800 Microplate Reader (Biohit) and protein concentration in each lysate was extrapolated from BSA dilutions standard curves.

Electrophoresis and western blot. Cell lysates (40 μg of protein in 1 : 4 volume of 5 × loading buffer (5% SDS, 25% 2-mercaptoethanol, 50% glycerol, 0.02% bromophenol blue and 0.04 M Tris)) were denatured at 60 °C for 1 h and electrophoretically separated by polyacrylamide gel electrophoresis on Mini-gel equipment (BioRad, Hemel Hempstead, UK). Prestained protein marker, Broad Range (7–175 kDa, New England BioLabs, Ipswich, MA, USA), diluted 1 : 3 in 1 × loading buffer, was used as marker.

Proteins were transferred to a polyvinylidene fluoride membrane for 90 min at a constant voltage of 100 V and in cold, stirred transfer buffer (25 mM Tris and 19.2 mM glycine). After blocking for 1 h at 4 °C in BB : PBS (1 : 1 dilution of Odyssey Blocking buffer (Li-Cor, Lincoln, NE, USA) in PBS), membranes were incubated with mouse anti-cleaved PARP (poly(ADP-ribose) polymerase; 1 : 8000 dilution, Cell Signaling, Hitching, UK) and rabbit anti-human β-tubulin (1 : 6000 dilution, Abcam, Cambridge, UK) antibodies overnight at 4 °C. Staining with secondary goat anti-mouse IRDye 800CW and goat anti-rabbit IRDye 680CW antibodies (both 1 : 10 000 dilution, Li-Cor) was followed by scanning on Li-Cor Odyssey Scanner (Li-Cor).

Analytical electrochemistry. To prepare solutions of analytes, 0.5 mg of solid sample was suspended in 1 ml of 100 mM tetrabutylammonium hexafluorophosphate dissolved in acetonitrile (MeCN), and the suspension was treated with ultrasound in a water bath (40 °C) for 30 min. Cyclic voltammograms were acquired using a Autolab PGStat (Eco-Chemie, Utrecht, Netherlands) at a scan rate of 100 $mV\,s^{-1}$, using only the tenth and final scan unless otherwise stated, to estimate the reduction potential of the analytes. A saturated calomel (Hg_2Cl_2) electrode was used as a reference and a fine platinum gauze (0.1 mm wire, 1 cm^2) as a counter electrode. A straight platinum wire (1 mm diameter) was used as a working electrode, and the experiments were carried out under a blanket of argon.

RNA processing, microarray hybridisation and data analysis. Raw and normalised gene expression files are available from the National Center for Biotechnology Information Gene Expression Omnibus (Barrett *et al*, 2005) under the accession number GSE70949.

Ten samples were collected comprising five breast cancer cell lines (MCF-7, MDA-MB-231, LCC1, LCC2 and LCC9) in two different conditions: untreated vehicle control (DMSO) and treated cells (6 h in 10 μM Oncamex). For this, 3×10^6 cells per cell line were treated, trypsinised and stored at −70 °C. The RNA was extracted using the Qiagen RNeasy Mini kit (Qiagen, Hilden, Germany), amplified and labelled using the Ambion Illumina TotalPrep RNA Amplification kit (Life, Carslbad, CA, USA) (in both steps as per the manufacturers' instructions) and hybridised to HumanHT-12 v4 Illumina BeadChips (Illumina, Cambridge, UK). Arrays were scanned using an Illumina iScan (Illumina).

Raw gene expression files were log2-transformed and quantile-normalised using the *lumi* Bioconductor package (Du *et al*, 2008), mapped to Ensembl gene identifiers and detection-filtered using re-annotation and pre-processing approaches previously described (Turnbull *et al*, 2012). Differential gene expression analysis was performed using pair-wise rank products (Breitling *et al*, 2004) between control and treated groups. Functional enrichment analysis of differentially expressed genes was performed using DAVID (Database for Annotation, Visualization and Integrated Discovery) Bioinformatics Resources 6.7 (Huang *et al*, 2009a, b). Heatmaps of differentially expressed genes belonging to clusters enriched for cell cycle and apoptosis were generated using log2 fold change expression values calculated between treated and control conditions for each cell line. Heatmaps were generated using TM4 microarray software suite's MultiExperiment Viewer (Saeed *et al*, 2003, 2006) and genes were ordered by Euclidean distance. Genes belonging to the apoptosis cluster were differentiated into pro- and anti-apoptosis clusters using Qiagen's custom referenced apoptosis PCR array literature (references therein).

Xenograft experiments. The xenograft studies were undertaken under a UK Home Office Project Licence in accordance with the Animals (Scientific Procedures) Act 1986, and studies were approved by the University of Edinburgh Animal Ethics Committee. The MDA-MB-231 xenografts were implanted subcutaneously into the flanks of adult (>8 weeks) female CD-1 immunodeficient mice (Charles River Laboratories, Tranent, UK), using 10 xenografts per experimental group of 6 mice, implanted in one or both flanks. Treatment was started when the mean tumour volume reached 0.25 cm^3 (day 0) and mice were treated daily intraperitoneally with Oncamex (25 $mg\,kg^{-1}$ per day) or with solvent control (10% DMSO in saline) on days 0–4 and 7–11. Changes in tumour size over 14 days were measured using Vernier callipers and volumes calculated ($V = l \times w^2/2$). Changes in mean body weight were recorded every 2 days over 14 days. The initial dose selection of 25 $mg\,kg^{-1}$ per day was based on the similarity of this structure to another compound for which 25 $mk\,kg^{-1}$ per day had been a safe dose. This dose was confirmed to be safe in an initial dose-testing experiment and no untoward effects were noted.

Immunohistochemistry. Xenograft tissue was collected, fixed in formalin and embedded in paraffin. Sections were dewaxed in xylene for 5 min and washed in alcohol and water before incubating in heated antigen retrieval solution (0.1 M sodium citrate and 0.1 M citric acid, pH 6). Slides were washed in PBS, incubated in 3% dH_2O_2 for 10 min and washed again in PBST (0.1% Tween-20 PBS) before incubating for 10 min in Total Protein Block (Dako, Ely, UK). Sections were incubated for 1 h in mouse monoclonal anti-Ki-67 antibody (1 : 300 dilution, Dako), followed by 30 min in Envision labelled polymer (Dako) and 10 min in DAB (1 : 50 dilution in buffer, Dako), with washes in PBST between each step. Finally, slides were counterstained in haematoxylin for 1 min and taken through graded alcohols to xylene before mounting in DPX mountant medium (Sigma-Aldrich, Dorset, UK).

Immunohistochemistry (IHC) scores were calculated by counting average positively stained cells across sections for each of the 10 xenografts for treated and control groups, using the average of calculations by three users to ensure unbiased estimations. Percentage of viability was assessed using the image-processing package Image J (NIH, Bethesda, MD, USA) to measure the viable areas in each section.

Other materials. Novel flavonoids tested (Table 1) were supplied by Antoxis Limited (Aberdeen, UK) from their library of proprietary compounds (Caldwell *et al*, 2007). They were custom synthesised and their purity was ascertained to be >95% by liquid

chromatography mass spectrometry and nuclear magnetic resonance. Unless otherwise stated, any other reagents and solvents were of analytical grade from Sigma-Aldrich and were used without further purification.

Statistical analysis. For analysis of SRB and other plate-based assays, all experiments were repeated at least once, and six technical replicates were used to calculate means and s.d. Results were processed, subtracting average values of blanks and day 0 controls and normalising to untreated controls. Cell proliferation curves were fitted to a model for sigmoidal regression using the Excel package Fit Designer 2D (IDBS, Guildford, UK), excluding outliers outside of a 95% confidence interval, for the calculation of half maximal inhibitory concentration (IC_{50}) values.

For statistical analysis of xenograft and IHC results, Prism 6 (GraphPad Software, La Jolla, CA, USA) was used to compare control and treated groups using unpaired *t*-test.

RESULTS

Novel flavonoid Oncamex exerts a potent antitumour effect in breast cancer cell lines. Among the eight compounds tested (Table 1) in a panel of SRB assays, AO-1530 and its second-generation methoxylated analogue Oncamex showed the strongest antiproliferative effects (Figure 1A and B). Oncamex was the most potent myricetin derivative of the series tested and exerted similar antiproliferative responses in MCF-7, BT-549, MDA-MB-231 and HBL-100 cells. For hormone-independent cell lines LCC1, LCC2 and LCC9, the two lead compounds were still more effective than myricetin although the overall effect was weaker.

Oncamex's IC_{50} values were between 4- and 140-fold lower than those of myricetin in all cell lines, while the potency and IC_{50} values of the other analogues were more variable (Figure 1C and D). Analogues AO-714A and AO-155-179 typically exerted antiproliferative effects closer to those of the lead compounds, whereas other analogues exerted weaker effects, with IC_{50} values closer to, or even higher, than those of myricetin.

Oncamex specifically targets the mitochondrial compartment, with rapid delivery and stable accumulation. Drug uptake and intracellular location was assessed by microscopic visualisation. Images obtained demonstrated a specific targeting of the mitochondrial compartment by Oncamex in the model breast cancer cell line MDA-MB-231 (selected for its better adherence when grown on coverslips; Figure 2). The compound was co-localised with Mitotracker (and absent from nuclei and cytoplasm) as early as 15 min after treatment and was still retained in the mitochondrial compartment after 6 h. Previous work in another cancer cell line has shown the ability of AO-1530 to target the mitochondria, whilst other analogues with weaker antiproliferative effects have less specific intracellular localisation (Supplementary Figure 2).

Oncamex exerts its antitumour effect through induction of cytotoxicity and apoptosis. Microscopic observation of MCF-7 cells showed that treatment with Oncamex induced substantial changes after 24 h, including a reduction of cell density and division, alterations in nuclear morphology and appearance of apoptotic cells (Figure 3A–D). By 72 h after treatment these changes were generalised, with abundant apoptotic, phagocytised and dead cells. These results suggested the involvement of apoptosis in Oncamex's mechanism of action.

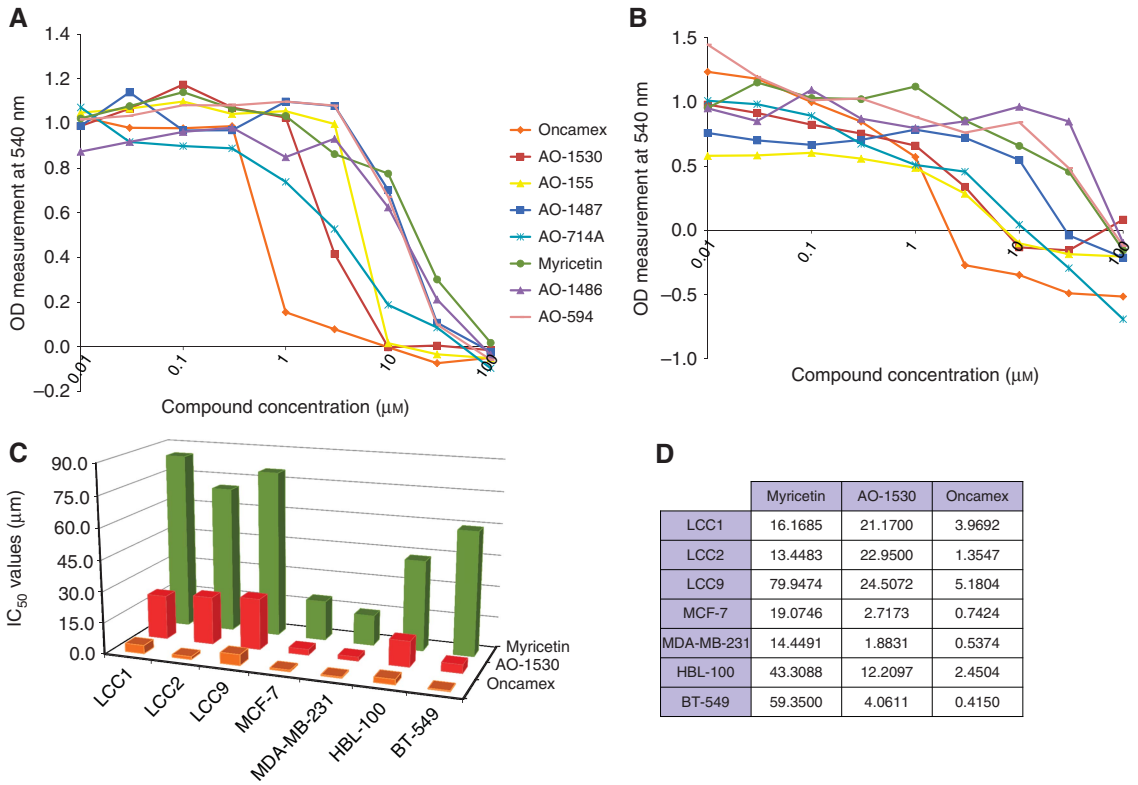

	Myricetin	AO-1530	Oncamex
LCC1	16.1685	21.1700	3.9692
LCC2	13.4483	22.9500	1.3547
LCC9	79.9474	24.5072	5.1804
MCF-7	19.0746	2.7173	0.7424
MDA-MB-231	14.4491	1.8831	0.5374
HBL-100	43.3088	12.2097	2.4504
BT-549	59.3500	4.0611	0.4150

Figure 1. Antitumour effect of Oncamex on breast cancer cell lines. The antiproliferative effect of a library of novel flavonoids was first assessed through SRB assays on a panel of seven breast cancer cell lines. Cells were treated for 4 days with drug concentrations in the 0.01–100 μM range concentration in all treatments. Results were comparable in all models, including MCF-7 (**A**) and MDA-MB-231 cells (**B**), with second-generation analogue Oncamex showing the strongest anticancer properties, markedly greater than those of myricetin. Analysis of concentration–response curves obtained from SRB assays allowed for the calculation of IC_{50} values for myricetin and the lead compounds (**C**, **D**), which reflected the stronger potency of Oncamex.

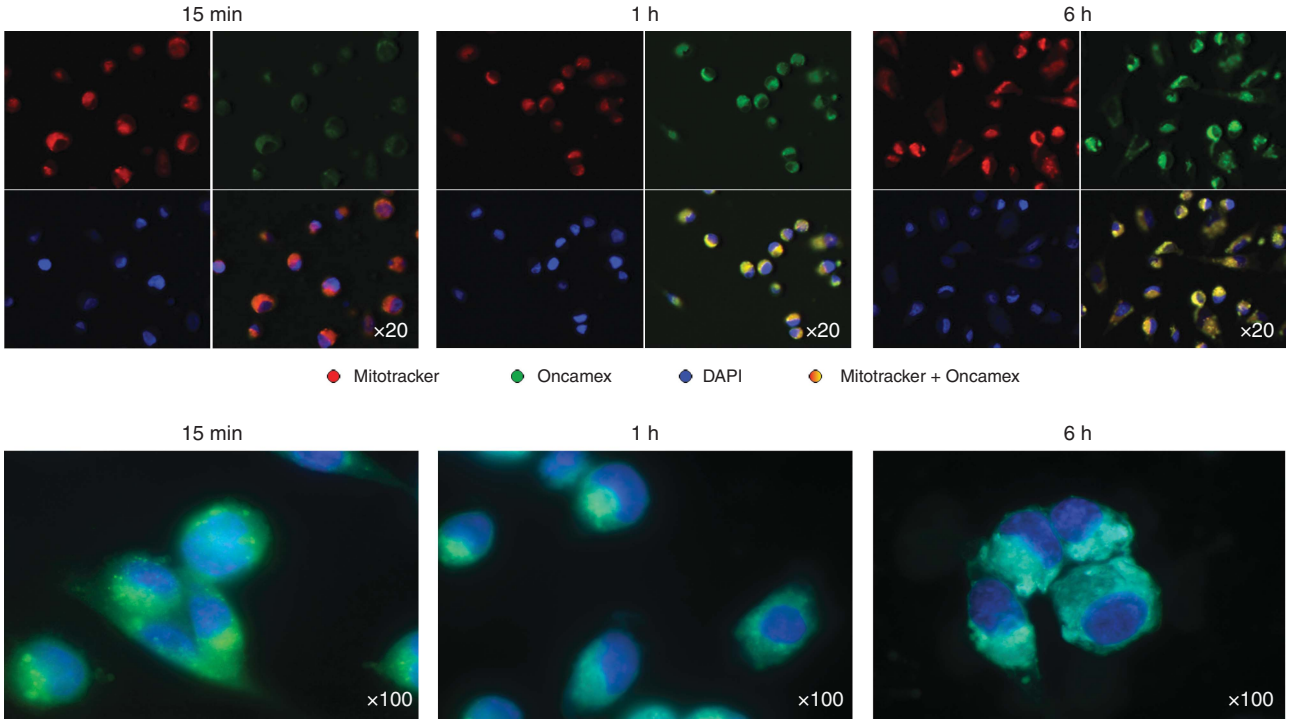

Figure 2. Intracellular localisation of Oncamex. Fluorescence microscopy on MDA-MB-231 cells treated with Oncamex demonstrated the rapid delivery of the drug and its localisation within the mitochondrial compartment, as shown by the overlap of the drug's fluorescent signal with that of Mitrotracker Deep Red (visualised as an orange–yellow signal resulting from the overlap of red and green fluorescences). The compound is delivered to the mitochondria as early as 15 min after the treatment and accumulates over time, retaining its organelle-specific targeting after 6 h. Visualisation of the cells at higher magnifications showed the change in cell morphology after 6 h, indicative of the induction of apoptosis.

SRB assays on cells exposed to different lengths of treatment (8, 16, 24, 48, 72 and 96 h) provided an insight into the timing of the anticancer effects observed (Supplementary Figure 3). Results showed that besides the more potent effect of Oncamex over AO-1530, the former also exerts a more rapid effect, inducing a significant reduction in cell density after 8 h comparable to the levels observed after 96 h, whereas AO-1530's effect was weaker and more delayed, not affecting cells until 24 h into treatment. CellTox plate assays showed that Oncamex produced an increase in cytotoxicity by 8 h after treatment in all cell lines (or earlier in some of them), reaching levels between 2- and 10-fold greater than the baseline signal by 24 h (Figure 3E).

Further investigation of Oncamex's mechanism of action using ApoTox multiplex assays showed that treatment of MCF-7, MDA-MB-231, HBL-100 and BT-549 cells with micromolar Oncamex concentrations for 8 h induced concentration-dependent, inversely correlated changes in cytotoxicity and cell viability, together with caspase-3/-7 activation, consistent with apoptosis (Figure 3G).

Induction of apoptosis was also measured by western blotting detection of PARP cleavage. Treatment with micromolar concentrations of AO-1530 or Oncamex led to cleavage of PARP. Oncamex exerted a more rapid effect, with cleaved PARP being detectable after 8 h, whereas 24-h incubation with AO-1530 was required for PARP cleavage to occur (Figure 3F).

ROS modulation is linked to Oncamex's properties. Oncamex displays an active redox profile. Analysis of electrochemical activity by cyclic voltammetry showed that Oncamex undergoes a reversible reduction, with a midpoint potential of $+145$ mV *vs* normal hydrogen electrode (Supplementary Figure 4).

To assess the role of ROS modulation in Oncamex's antitumour effect, ApoTox assays were repeated with the addition of a 30-min pre-incubation stage using an antioxidant agent (5 or 10 mM *N*-acetyl cysteine, NAC). Results with both model cell lines used (MCF-7 and MDA-MB-231, selected to include both an ER-positive and a triple-negative cell line, respectively) showed pre-treatment with 10 mM NAC caused a partial, but not complete, blockage of the cytotoxic and apoptotic signals induced by treatment with Oncamex (Figure 3H).

To investigate the effect of Oncamex on ROS production, MDA-MB-231 cells (selected for their better adherence when grown on coverslips) were stained with the novel fluorescent probes MitoPY1 or MitoSOX for the specific detection of mitochondrial hydrogen peroxide (mH_2O_2) and superoxide (mSO), respectively. The signal generated by MitoPY1 was not intense enough to allow for sensitive quantification, but provided qualitative results in the form of bright specks localised in the mitochondrial department. The induction of mH_2O_2 was observed 1 h after treatment with 0.3 μM Oncamex but no significant signals arose after longer incubations (Figure 4A). MitoSOX results showed a quantifiable, significant increase in mSO production in cells treated with higher concentrations of Oncamex for longer treatment times (Figure 4B and C).

Oncamex induces gene expression changes related to cell cycle and apoptosis regulation. Results from microarray experiments showed that 6-h treatment with Oncamex altered the expression profile of genes related to cell cycle and apoptosis (Figure 5). Genes involved in cell cycle regulation were downregulated by treatment in all cell lines studied. These include genes encoding proteins with well-known biological functions such as cyclins (encoded by *CCND1*, *CCNF* or *CCNB1*), regulators of proliferation (*AURKA* and *MKI67*) and other cell division-promoting proteins (*CDC20*, *MCM5* or *MCM3*).

Functional enrichment analysis showed that Oncamex induces different effects in two clusters of apoptosis-related genes. Pro-apoptotic genes were upregulated by treatment, including genes encoding apoptosis-inducing proteins (such as *BNIP3*,

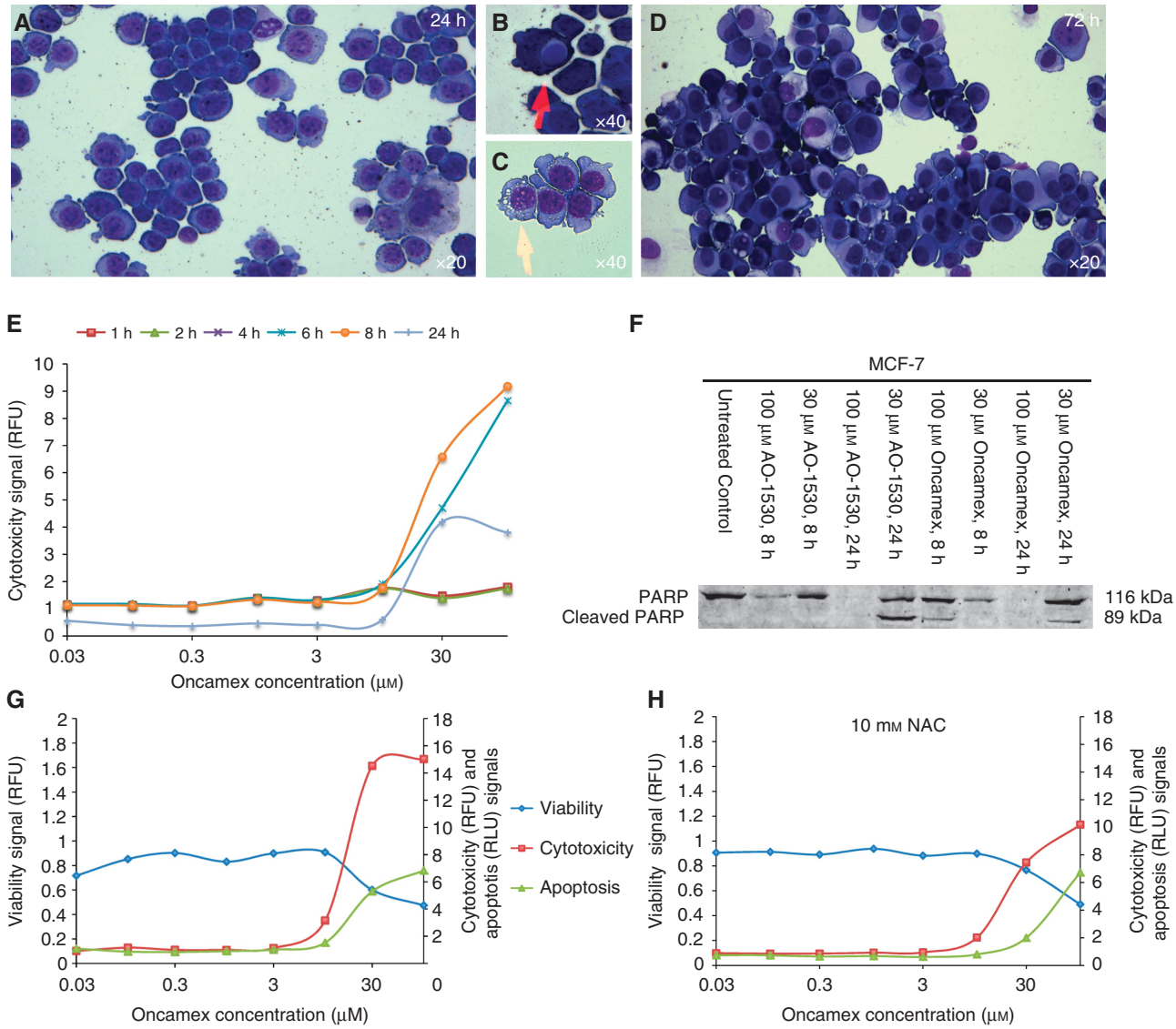

Figure 3. Cytotoxic and apoptotic effects of Oncamex. Initial evidence on the mechanism of action of Oncamex was obtained from study of breast cancer cell line models MCF-7 and MDA-MB-231. Microscopic visualisation of MCF-7 cells treated with 30 µM Oncamex showed a reduction in cell density, changes in cell morphology and the appearance of apoptotic and dead cells after 24 h (**A–C**), which was generalised by 72 h after treatment (**D**). CellTox Green plate assays supported preliminary results by direct measurement of the induction of cytotoxicity in treated MDA-MB-231 cells, peaking 8 h after treatment (**E**). Western blotting was used to measure PARP cleavage in treated MCF-7 cells (**F**): Oncamex seemed to induce apoptosis faster, with PARP cleavage occurring after 8 h treatment with the highest concentrations, whereas 24-h incubation was required with AO-1530. The 24-h incubation with the highest concentrations seemed to induce further cell degradation, preventing protein detection. Apoptosis was confirmed by an additional method using ApoTox plate assays, which reported an dose-dependent increase in cytotoxicity and apoptosis, inversely proportional to cell viability (**G**). These antitumour effects were partially blocked by 30 pre-treatment with 10 mM of the antioxidant NAC (**H**).

BNIP3L or *CRADD*) and caspases (*CASP7*). Anti-apoptotic genes were downregulated, including decreased expression of genes involved in apoptosis inhibition (*DFFA*, *BCL2*, *BIRC6* or *BIRC5*) or survival and proliferation (*IL10*).

Oncamex inhibits tumour proliferation and viability in a mouse *in vivo* model. Results from a first *in vivo* model in mice implanted with MDA-MB-231 xenografts (selected for the better ability of these cells to grow as xenografts) showed that treatment with Oncamex (25 mg kg^{-1} per day) had a significant effect ($P<0.05$), inhibiting tumour growth as indicated by changes in xenograft volume compared with untreated mice (Figure 6A). Treatment did not entail significant changes in mean body weight (<4% loss over 20 days) (Figure 6B).

IHC processing of collected xenograft tissue identified a significant decrease in Ki-67 expression, from 60% in controls to 36% in mice treated with Oncamex (Figure 6C–F), suggesting that this compound inhibits cell proliferation *in vivo*. Similarly, the percentage of viable areas was significantly reduced from 56 to 37% (Figure 6C–E and G).

DISCUSSION

In this study, we have identified several novel flavonoids with greater potency than myricetin when assessed in a panel of seven breast cancer cell lines. AO-1530, a synthetic analogue of myricetin

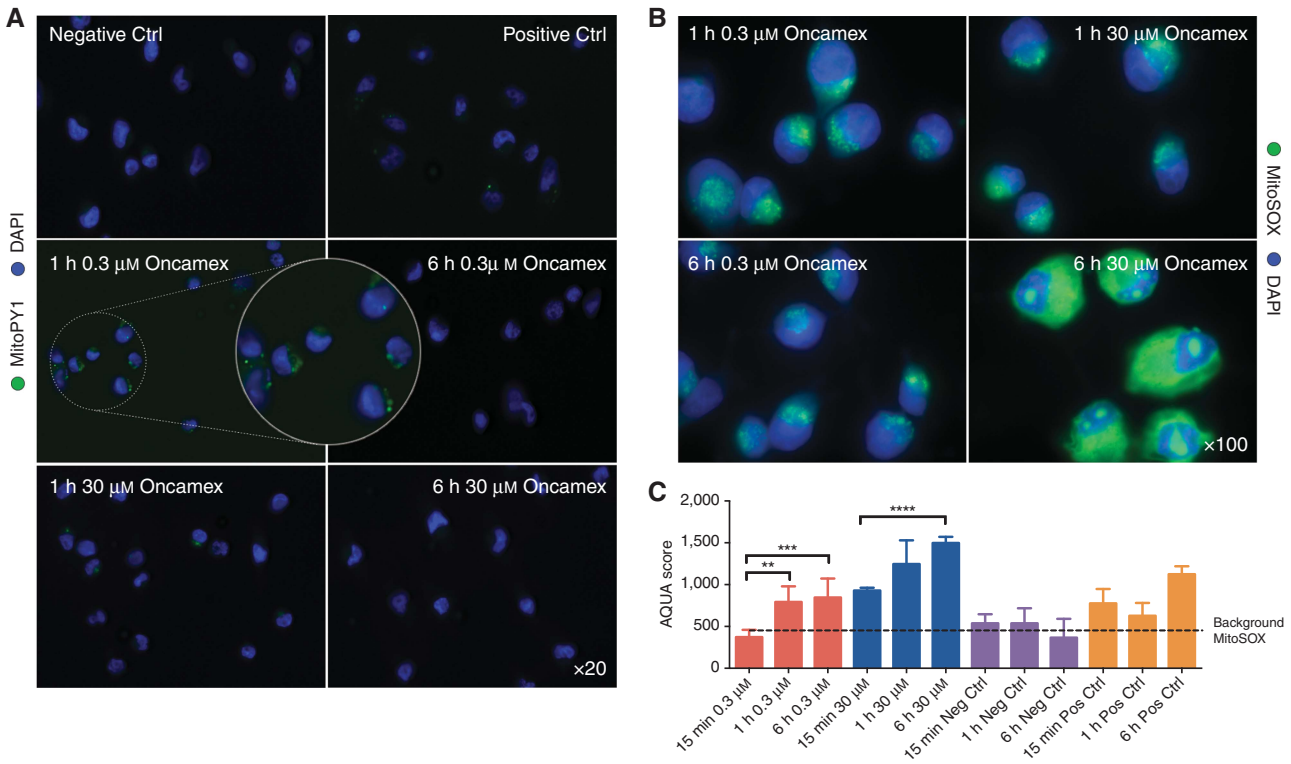

Figure 4. Effect of Oncamex on production of mitochondrial ROS. The production of ROS in MDA-MB-231 cells exposed to Oncamex in different treatment conditions was assessed using mitochondrial, species-specific fluorescent probes for microscopic visualisation of production of different species *in situ*. MitoPY1 produced a signal too weak for reliable quantification, but provided qualitative results showing an increase in mH_2O_2 after short incubations with 0.3 μM Oncamex (**A**), visible as bright specks in the mitochondrial compartment similar to the ones observed in the positive control treated with 100 μM H_2O_2. Measurement of MitoSOX reported a quantifiable, significant increase in mSO 6 h after treatment with 30 μM Oncamex (**B**), as supported by statistical analysis of measurements (**C**). *P*-values from unpaired *t*-test: $^{**}P<0.01$; $^{***}P<0.001$; $^{****}P<0.0001$. Where not shown $P>0.05$ (nonsignificant).

in which the non-redox-active OH groups on the A-ring of the flavonoid have been removed and a decyl chain has been added to improve cell membrane permeability (analogous to the function of the chain in vitamin E), had previously been identified as a more potent antioxidant than myricetin (McPhail *et al*, 2009). Results from SRB assays have indicated that AO-1530's strong antiproliferative properties are surpassed by Oncamex, a second-generation bi-methoxylated analogue.

We aimed to identify the SAR properties contributing to the stronger potency of these novel analogues. The library of compounds studied included molecules specifically designed to achieve distinct intracellular targeting and effective redox properties. One of the defining characteristics of Oncamex is the inclusion of two methoxy moieties in its structure. Previous research has suggested contrasting effects of methoxy substitutions in chemical entities: it has been reported that they may have unfavourable steric effects, compromising redox-modulating and cytochrome P450 (CYP1)-inhibitory capabilities (Heim *et al*, 2002; Arroo *et al*, 2009), while the extent of the BCRP-inhibitory properties of flavonoids also depends on the number and location of these modifications (Katayama *et al*, 2007; Pick *et al*, 2011; Tan *et al*, 2013). Nevertheless, the enhanced potency of Oncamex is most likely the result of methoxylation leading to improved pharmacokinetic properties and increased stability: methoxylated compounds are less prone to modifications such as glucuronidation and sulphation, and are thus more chemically and metabolically stable (Androutsopoulos *et al*, 2010). Added to improved uptake and membrane transport, such alterations may provide these compounds with increased bioavailability (Walle, 2007; Arroo *et al*, 2009). Moreover, it has been reported that upon delivery, methoxylated compounds are targeted by tumour-specific *O*-demethylases that provide free hydroxyl groups and hence an increase in redox properties (Androutsopoulos *et al*, 2008; Arroo *et al*, 2009). Therefore, it seems reasonable that chain-bearing, methoxylated novel flavonoids could make promising candidates as potential chemotherapeutic agents, providing improved pharmacological attributes, including cancer-specific activation.

Although Oncamex was the most potent compound in this series, the effect of the other analogues was more variable. Interestingly, the fully methoxylated molecule AO-714A showed a potent effect with variable but generally low IC_{50} values. This also supports the notion that flavonoids may not require free hydroxyl groups to be active anticancer agents due to their propensity to undergo demethylation *in vivo* by *O*-demethylases (Arroo *et al*, 2009). Similar to Oncamex, AO-714A presents multiple methoxylations that would improve its bioavailability and these are located in the 3′, 4′ and 5′ positions, reported as structural features that significantly increase the BCRP-inhibitory activity of flavonoids (Katayama *et al*, 2007; Tan *et al*, 2013). These observations suggest that different mechanisms such as induction of oxidative phosphorylation-independent cell death (as previously reported with myricetin (Ko *et al*, 2005b)) could also be relevant to their anticancer effect. Finally, other analogues expected to have a redox potential comparable to that of AO-1530 but with no specific targeting for mitochondria showed lower potency, highlighting the importance of targeted drug delivery.

Overall, these results indicate that particular SARs are relevant for the application of flavonoids to cancer treatment. The antitumour effect of these novel molecules is most likely the result of a combination of different structural traits and properties,

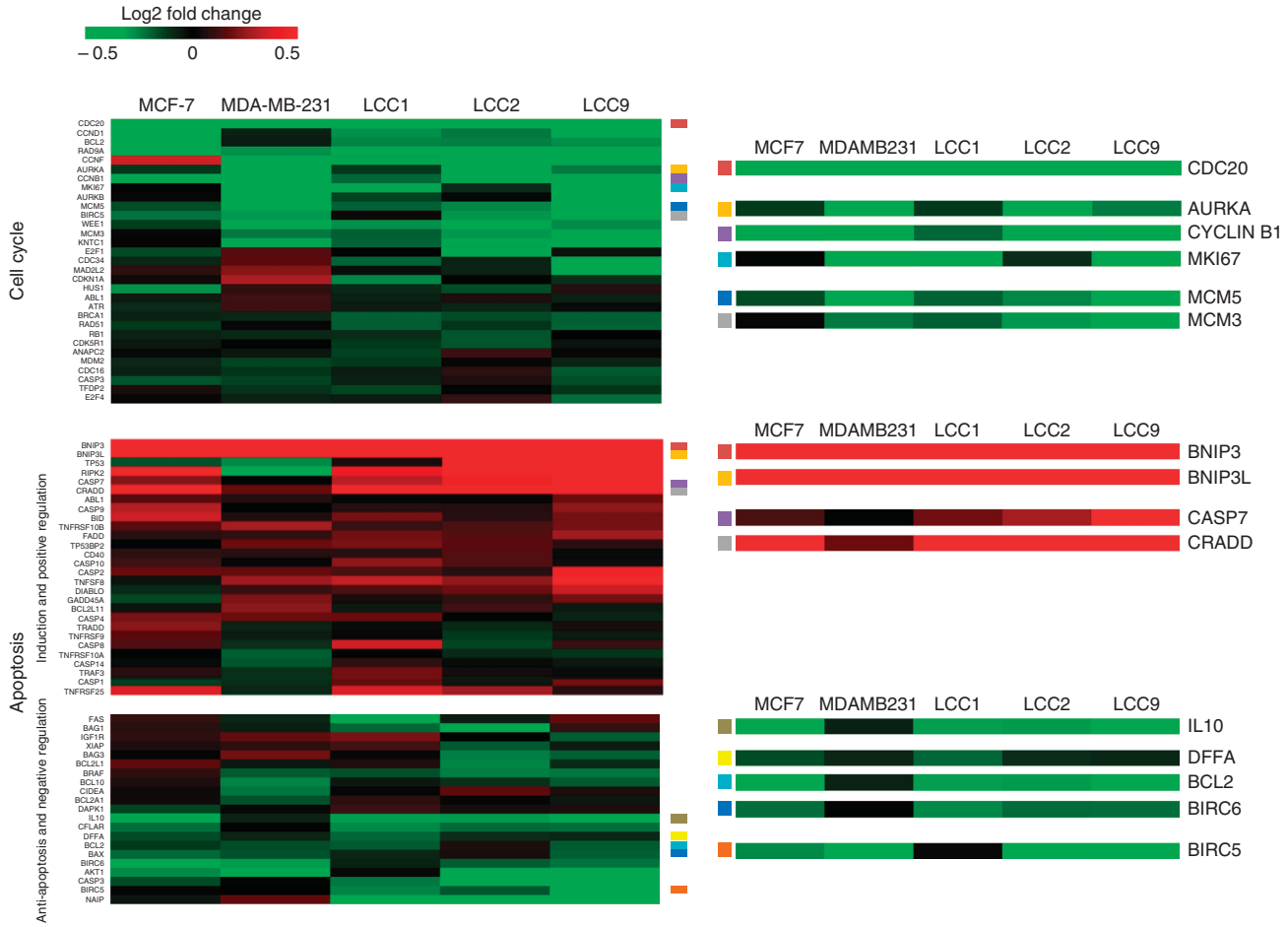

Figure 5. Modulation of gene expression by treatment with Oncamex. Heatmaps based on log2 fold changes between control and treated (6 h 10 μM Oncamex) summarising changes in gene expression in cell cycle and apoptosis function groups. Red and green represent high and low log2 gene expression fold changes, respectively. Genes are ordered by Euclidean distance. Representative examples of well-characterised genes in each pathway, which are up- or downregulated the most on treatment, are enlarged in panels to the right and their position in the overall heatmap is indicated by colour-coded markers.

including optimum redox potential and structural resemblance to the flavonoid backbone, which has been shown to allow for a wide range of molecular interactions for different polyphenols (Martinez-Perez *et al*, 2014). In addition, the substitution with electron-donating moieties, methoxylated residues and mitochondrial targeting provide significantly stronger antitumour properties.

Oncamex exerts an antiproliferative effect on cancer cells and has been found to induce apoptosis, as suggested by the development of responses as soon as 8 h after treatment by detection of caspase activation and PARP cleavage. Results from the panel of breast cancer cell lines studied suggest that the antitumour effect of Oncamex is independent of ER status, as triple-negative cell lines MDA-MB-231, BT-549 and HBL-100 cells showed susceptibility similar to that of ER-positive cells. This suggests that Oncamex's effect does not rely on modulation of hormonal signals and thus may be applicable to cancers of a more varied nature. We observed that LCC cell lines, which are ER-positive but hormone-independent MCF-7 variants, are less sensitive to Oncamex, but this is most likely due to the lower baseline proliferation rate of LCC cells (Brünner *et al*, 1993a, b, 1997).

The cytotoxic and apoptotic signals induced by Oncamex were partially blocked by pre-incubation with an antioxidant, suggesting that the compound's redox activity, studied by electrochemical analysis, is at least partially involved in the induction of these responses through ROS modulation. The production of ROS was detected by fluorescence microscopy using species-specific probes to obtain *in situ* visualisation. Results reported the induction of different mitochondrial ROS production in a concentration- and time-dependent manner. Whereas mH_2O_2 was produced shortly after treatment with nanomolar concentrations of Oncamex, mSO was produced after 6 h treatment with higher concentrations, in the same timeframe and concentration range linked to Oncamex's antitumour properties. The redox profile for Oncamex showed that it undergoes a reversible reduction with a midpoint potential of $+145$ mV, a value substantially more positive than the physiological resting redox potential in either cytoplasm or mitochondria (Auchinvole *et al*, 2012; Mallikarjun *et al*, 2012). This supports the notion that although aspects such as kinetics and biostability may affect its reactivity, Oncamex would most likely be found in its reduced form in the mitochondrial compartment and thus be able to donate an electron to oxygen to form the superoxide radical anion. Hence, results obtained from the study of mitochondrial ROS suggest that production of superoxide in the mitochondrial compartment might be associated with the antitumour effects exerted but also support the existence of a biphasic effect, previously reported for polyphenols such as flavonoids (Ramos, 2007), by which different, possibly opposing effects might be exerted by a compound depending on a fine concentration balance.

Gene expression analysis was carried out to study the effect of Oncamex on breast cancer cell line models at gene expression level.

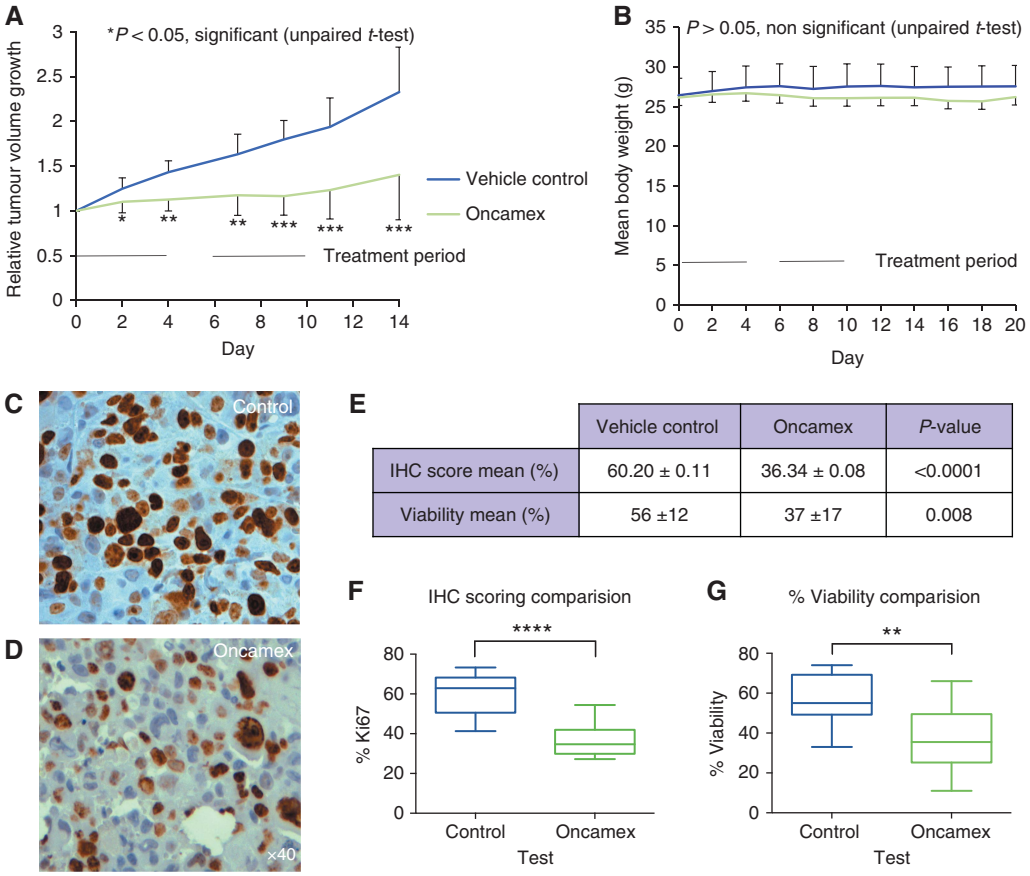

	Vehicle control	Oncamex	*P*-value
IHC score mean (%)	60.20 ± 0.11	36.34 ± 0.08	<0.0001
Viability mean (%)	56 ±12	37 ±17	0.008

Figure 6. Effect of Oncamex on xenografts in an *in vivo* mice model. Treatment of mice implanted with MDA-MB-231 xenografts with Oncamex (25 mg kg^{-1} per day, treating for 4 consecutive days with a 2-day rest in between) showed to exert a significant growth-inhibitory effect in comparison to untreated animals (**A**). Mean body weight was registered every second day for 20 days (**B**). Ki-67 activation was measured by immunohistochemistry in controls (**C**) and xenografts treated with Oncamex (**D**). Statistical study reported a statistically significant decrease in expression of the proliferation-linked protein as reported unpaired *t*-test analysis (**E**, **F**). Image analysis with the open-access processing programme ImageJ also showed a statistically significant reduction in the percentage of viable areas in the tissue (**E**, **G**). *P*-values from unpaired *t*-test: *$P<0.05$; **$P<0.01$; ***$P<0.001$; ****$P<0.0001$. Where not shown $P>0.05$ (nonsignificant).

Cells were exposed to treatment levels that had been shown to exert changes in proliferation and cell death, as well as to induce changes in ROS signalling. Results supported the antiproliferative and pro-apoptotic effects previously measured using cytotoxicity assays, western blotting and different plate assays. This suggests that the rapid delivery of Oncamex to the mitochondria is also translated either directly or indirectly into regulation of these pathways at gene expression level. Importantly, Oncamex induced largely the same effect across different cell lines despite their inherent biological differences.

The ROS status has been established as a major regulator in the development and advancement of cancer and, as the site of cell respiration, the mitochondrial compartment is the main source of ROS-linked signalling. Hence, a number of different mechanisms could be altered by the effect of these ROS-modulating drugs in the mitochondria. Given the versatility of flavonoids as anticancer agents, these results show that while Oncamex's promise as an antitumour agent has been demonstrated, its mechanism of action is probably complex and further study will be required for a better understanding.

Oncamex demonstrated significant growth-inhibitory activity in the MDA-MB-231 breast cancer xenograft model at a dose level that was not associated with any indications of toxicity. The proliferative marker Ki-67 was reduced by treatment with the drug consistent with an antiproliferative effect. Further studies are now required to observe whether other breast cancer xenografts are sensitive to this drug and to further study the pharmacokinetic and pharmacodynamic properties of this agent.

In conclusion, we have shown the potential of the prototypic novel compound Oncamex as an antitumour agent. This suggests that myricetin's natural scaffold can be modified to enhance its activity and shows the potential for mitochondrial targeted, redox-active molecules in cancer therapy. The results reported in this study have provided evidence of the anticancer effect of Oncamex in *in vitro* cell culture models, as well as preliminary antitumour activity in an *in vivo* xenograft model in mice.

ACKNOWLEDGEMENTS

We are grateful to Professor Robert Clarke for the use of the LCC1, LCC2 and LCC9 cell lines; to Sonya Uddin and Chrysi Xintaropoulou for their help with the gene extraction procedures; to Paul Perry for his assistance with microscopy; and to Helen Caldwell and Elaine McLay for sectioning of formalin-fixed and paraffin-embedded tissues. We thank SULSA (Scottish Universities Life Science Alliance) for supporting this project through a SULSA BioSkape Industry PhD Studentship and Antoxis Limited for providing additional funding. We also thank the Seventh Framework Programme of the European Union (METOXIA project; HEALTH-F2-2009-222741) for support.

CONFLICT OF INTEREST

DM and GC are employees of Antoxis Limited. The remaining authors declare no conflict of interest.

AUTHOR CONTRIBUTIONS

CM-P, CW, DJH, DM and SPL conceived of the study and participated in its design and coordination, and helped to draft the manuscript; CM-P, AKT, JM and EJJ participated in the gene extraction and IHC procedures; PM and CW assisted with cell culture; GC assisted with microscopy; PITT and CJC assisted with analytical electrochemistry and participated in cyclic voltammetry experiments; DM, PITT and CJC provided guidance on chemistry and ROS biology; CM-P and AKT carried out the gene expression analysis; SPL carried out the *in vivo* experiments; all authors contributed to and approved the final manuscript.

REFERENCES

Androutsopoulos V, Arroo RRJ, Hall JF, Surichan S, Potter GA (2008) Antiproliferative and cytostatic effects of the natural product eupatorin on MDA-MB-468 human breast cancer cells due to CYP1-mediated metabolism. *Breast Cancer Res* **10**: R39.

Androutsopoulos VP, Papakyriakou A, Vourloumis D, Tsatsakis AM, Spandidos DA (2010) Dietary flavonoids in cancer therapy and prevention: substrates and inhibitors of cytochrome P450 CYP1 enzymes. *Pharmacol Ther* **126**: 9–20.

Arroo RRJ, Androutsopoulos V, Beresford K, Ruparelia K, Surichan S, Wilsher N, Potter GA (2009) Phytoestrogens as natural prodrugs in cancer prevention: dietary flavonoids. *Phytochem Rev* **8**: 375–386.

Auchinvole CAR, Richardson P, McGuinnes C, Mallikarjun V, Donaldson K, McNab H, Campbell CJ (2012) Monitoring intracellular redox potential changes using SERS nanosensors. *ACS Nano* **6**: 888–896.

Barrett T, Suzek TO, Troup DB, Wilhite SE, Ngau W-C, Ledoux P, Rudnev D, Lash AE, Fujibuchi W, Edgar R (2005) NCBI GEO: mining millions of expression profiles—database and tools. *Nucleic Acids Res* **33**: D562–D566.

Breitling R, Armengaud P, Amtmann A, Herzyk P (2004) Rank products: a simple, yet powerful, new method to detect differentially regulated genes in replicated microarray experiments. *FEBS Lett* **573**: 83–92.

Brown DM, Kelly GE, Husband A (2005) Flavonoid compounds in maintenance of prostate health and prevention and treatment of cancer. *Mol Biotechnol* **30**: 253–270.

Brünner N, Boulay V, Fojo A (1993a) Acquisition of hormone-independent growth in MCF-7 cells is accompanied by increased expression of estrogen-regulated genes but without detectable DNA amplifications. *Cancer Res* **53**: 283–290.

Brünner N, Boysen B, Jirus S, Brunner N, Frandsen T, Spang-thomsen M, Skaar TC, Hoist-hansen C, Fuqua SAW (1997) MCF7/LCC9: an antiestrogen-resistant MCF-7 variant in which acquired resistance to the steroidal antiestrogen ICI 182, 780 confers an early cross-resistance to the nonsteroidal antiestrogen tamoxifen. *Cancer Res* **57**: 3486–3493.

Brünner N, Frandsen TL, Holst-hansen C, Brãnner N, Lippman ME, Clarke R, Bei M, Thompson EW, Wakeling AE (1993b) MCF7/LCC2: a 4-hydroxytamoxifen resistant human breast cancer variant that retains sensitivity to the steroidal antiestrogen ICI 182, 780. *Cancer Res* **53**: 3229–3232.

Caldwell ST, Bennett CJ, Hartley RC, McPhail DB, Duthie GG (2007) Flavonoid compounds as therapeutic antioxidants. Patent no. WO 2004/007475 A1.

Ciolino HP, Yeh GC (1999) Inhibition of aryl hydrocarbon-induced cytochrome P-450 1A1 enzyme activity and CYP1A1 expression by resveratrol. *Mol Pharmacol* **56**: 760–767.

Du P, Kibbe WA, Lin SM (2008) lumi: a pipeline for processing Illumina microarray. *Bioinformatics* **24**: 1547–1548.

Harris DM, Besselink E, Henning SM, Go VLW, Heber D (2005) Phytoestrogens induce differential estrogen receptor alpha- or beta-mediated responses in transfected breast cancer cells. *Exp Biol Med* **230**: 558–568.

Heim KE, Tagliaferro AR, Bobilya DJ (2002) Flavonoid antioxidants: chemistry, metabolism and structure-activity relationships. *J Nutr Biochem* **13**: 572–584.

Huang DW, Sherman BT, Lempicki RA (2009a) Bioinformatics enrichment tools: paths toward the comprehensive functional analysis of large gene lists. *Nucleic Acids Res* **37**: 1–13.

Huang DW, Sherman BT, Lempicki RA (2009b) Systematic and integrative analysis of large gene lists using DAVID bioinformatics resources. *Nat Protoc* **4**: 44–57.

Katayama K, Masuyama K, Yoshioka S, Hasegawa H, Mitsuhashi J, Sugimoto Y (2007) Flavonoids inhibit breast cancer resistance protein-mediated drug resistance: transporter specificity and structure-activity relationship. *Cancer Chemother Pharmacol* **60**: 789–797.

Ko C-H, Shen S-C, Lee TJF, Chen Y-C (2005a) Myricetin inhibits matrix metalloproteinase 2 protein expression and enzyme activity in colorectal carcinoma cells. *Mol Cancer Ther* **4**: 281–290.

Ko CH, Shen S-C, Hsu C-S, Chen Y-C (2005b) Mitochondrial-dependent, reactive oxygen species-independent apoptosis by myricetin: roles of protein kinase C, cytochrome c, and caspase cascade. *Biochem Pharmacol* **69**: 913–927.

Limer JL, Speirs V (2004) Phyto-oestrogens and breast cancer chemo-prevention. *Breast Cancer Res* **6**: 119–127.

Mai Z, Blackburn GL, Zhou J (2007) Genistein sensitizes inhibitory effect of tamoxifen on the growth of estrogen receptor-positive and HER2-overexpressing human breast cancer cells. *Mol Carcinog* **46**: 534–542.

Mallikarjun V, Clarke DJ, Campbell CJ (2012) Cellular redox potential and the biomolecular electrochemical series: a systems hypothesis. *Free Radic Biol Med* **53**: 280–288.

Martinez-Perez C, Ward C, Cook G, Mullen P, McPhail D, Harrison DJ, Langdon SP (2014) Novel flavonoids as anti-cancer agents: mechanisms of action and promise for their potential application in breast cancer. *Biochem Soc Trans* **42**: 1017–1023.

McCarty MF (2006) Isoflavones made simple - Genistein's agonist activity for the beta-type estrogen receptor mediates their health benefits. *Med Hypotheses* **66**: 1093–1114.

McPhail DB, Cook GJ, Johnstone AS, Docherty K (2009) Protection of mESCs from oxidative stress-induced cell death by a novel class of mitochondrial-targeted, high-potency antioxidant. *British Pharmacological Society Summer Meeting 2009 Abstract*.

Moon YJ, Wang X, Morris ME (2006) Dietary flavonoids: effects on xenobiotic and carcinogen metabolism. *Toxicol In Vitro* **20**: 187–210.

Pan H, Zhou W, He W, Liu X, Ding Q, Ling L, Zha X, Wang S (2012) Genistein inhibits MDA-MB-231 triple-negative breast cancer cell growth by inhibiting NF-κB activity via the Notch-1 pathway. *Int J Mol Med* **30**: 337–343.

Park KI, Park HS, Nagappan A, Hong GE, Lee DH, Kang SR, Kim JA, Zhang J, Kim EH, Lee WS, Shin SC, Hah YS, Kim GS (2012) Induction of the cell cycle arrest and apoptosis by flavonoids isolated from Korean Citrus aurantium L. in non-small-cell lung cancer cells. *Food Chem* **135**: 2728–2735.

Peluso I, Raguzzini A, Serafini M (2013) Effect of flavonoids on circulating levels of TNF-α and IL-6 in humans: a systematic review and meta-analysis. *Mol Nutr Food Res* **57**: 784–801.

Pick A, Müller H, Mayer R, Haenisch B, Pajeva IK, Weigt M, Bönisch H, Müller CE, Wiese M (2011) Structure-activity relationships of flavonoids as inhibitors of breast cancer resistance protein (BCRP). *Bioorg Med Chem* **19**: 2090–2102.

Ramos S (2007) Effects of dietary flavonoids on apoptotic pathways related to cancer chemoprevention. *J Nutr Biochem* **18**: 427–442.

Rice S, Whitehead SA (2006) Phytoestrogens and breast cancer – promoters or protectors? *Endocr Relat Cancer* **13**: 995–1015.

Romano B, Pagano E, Montanaro V, Fortunato AL, Milic N, Borrelli F (2013) Novel insights into the pharmacology of flavonoids. *Phytother Res* **27**: 1588–1596.

Saeed AI, Bhagabati NK, Braisted JC, Liang W, Sharov V, Howe EA, Li J, Thiagarajan M, White JA, Quackenbush J (2006) TM4 microarray software suite. *Methods Enzymol* **411**: 134–193.

Saeed AI, Sharov V, White J, Li J, Liang W, Bhagabati N, Braisted J, Klapa M, Currier T, Thiagarajan M, Sturn A, Snuffin M, Rezantsev A, Popov D, Ryltsov A, Kostukovich E, Borisovsky I, Liu Z, Vinsavich A, Trush V, Quackenbush J (2003) TM4: a free, open-source system for microarray data management and analysis. *Biotechniques* **34**: 374–378.

Sanderson JT, Hordijk J, Denison MS, Springsteel MF, Nantz MH, van den Berg M (2004) Induction and inhibition of aromatase (CYP19) activity by natural and synthetic flavonoid compounds in H295R human adrenocortical carcinoma cells. *Toxicol Sci* **82**: 70–79.

Siegelin MD, Gaiser T, Habel A, Siegelin Y (2009) Myricetin sensitizes malignant glioma cells to TRAIL-mediated apoptosis by down-regulation of the short isoform of FLIP and bcl-2. *Cancer Lett* **283**: 230–238.

Singh N, Zaidi D, Shyam H, Sharma R, Balapure AK (2012) Polyphenols sensitization potentiates susceptibility of MCF-7 and MDA MB-231 cells to Centchroman. *PLoS One* **7**: e37736.

Ström A, Hartman J, Foster JS, Kietz S, Wimalasena J, Gustafsson J-Å (2004) Estrogen receptor β inhibits 17β-estradiol-stimulated proliferation of the breast cancer cell line T47D. *Proc Natl Acad Sci USA* **101**: 1566–1571.

Tan KW, Li Y, Paxton JW, Birch NP, Scheepens A (2013) Identification of novel dietary phytochemicals inhibiting the efflux transporter breast cancer resistance protein (BCRP/ABCG2). *Food Chem* **138**: 2267–2274.

Thompson EW, Brünner N, Torri J, Johnson MD, Boulay V, Wright A, Lippman ME, Steeg PS, Clarke R (1993) The invasive and metastatic properties of hormone-independent but hormone-responsive variants of MCF-7 human breast cancer cells. *Clin Exp Metastasis* **11**: 15–26.

Tu S-H, Ho C-T, Liu M-F, Huang C-S, Chang H-W, Chang C-H, Wu C-H, Ho Y-S (2013) Luteolin sensitises drug-resistant human breast cancer cells to tamoxifen via the inhibition of cyclin E2 expression. *Food Chem* **141**: 1553–1561.

Turnbull AK, Kitchen RR, Larionov AA, Renshaw L, Dixon JM, Sims AH (2012) Direct integration of intensity-level data from Affymetrix and Illumina microarrays improves statistical power for robust reanalysis. *BMC Med Genomics* **5**: 35.

Walle T (2007) Methylation of dietary flavones greatly improves their hepatic metabolic stability and intestinal absorption. *Mol Pharm* **4**: 166–170.

Weng C-J, Yen G-C (2012) Flavonoids, a ubiquitous dietary phenolic subclass, exert extensive in vitro anti-invasive and in vivo anti-metastatic activities. *Cancer Metastasis Rev* **31**: 323–351.

Yi T, Li H, Wang X, Wu Z (2008) Enhancement radiosensitization of breast cancer cells by deguelin. *Cancer Biother Radiopharm* **23**: 355–362.

Zhang Q, Zhao X-H, Wang Z-J (2008) Flavones and flavonols exert cytotoxic effects on a human oesophageal adenocarcinoma cell line (OE33) by causing G2/M arrest and inducing apoptosis. *Food Chem Toxicol* **46**: 2042–2053.

Supplementary Information accompanies this paper on British Journal of Cancer website (http://www.nature.com/bjc)